

Preparation and *in vitro* antibacterial activity against *Pantoea stewartii* causing jackfruit bronzing disease of nano ZnO/oligochitosan-iodine complex

Bui Duy Du^{1,2}, Nguyen Trong Hoanh Phong^{2,*}, Le Nghiem Anh Tuan^{1,*},
Tran Phuoc Tho¹, Nguyen Quoc Hien¹

¹Institute of Applied Materials Science, Vietnam Academy of Science and Technology, No. 1B,
TL29 Street, Thanh Loc ward, District 12, Ho Chi Minh City 700000, Viet Nam.

²Graduate University of Science and Technology, Vietnam Academy of Science and Technology,
No. 18 Hoang Quoc Viet Street, Cau Giay District, Hanoi 100000, Viet Nam.

*Email: sharahio@yahoo.com; lenghiemanhtuan@gmail.com;

Received: 4 July 2023; Accepted for publication: 18 October 2024

Abstract. Nano ZnO/oligochitosan (nano ZnO/OC) and nano ZnO/oligochitosan-iodine (nano ZnO/OC-I₂) complex prepared in this study were new materials consisting of nano ZnO (12.3 - 15.0 nm) dispersed in OC and OC-I₂ solutions. Both nano ZnO/OC and nano ZnO/OC-I₂ exhibited resistance to *P. stewartii*, which causes jackfruit bronzing disease. The OC with a low molecular weight (Mw) of about 3,300 g/mol had the main advantage of complete solubility in both acidic and alkaline mediums up to pH 9. The studied materials were characterized by gel permeation (GPC) chromatography, proton nuclear magnetic resonance (¹H-NMR), transmission electron microscopy (TEM) and X-ray diffraction (XRD). The results of the *in vitro* test against *Pantoea stewartii* of nano ZnO/OC-I₂ showed that the antibacterial efficacy attained to 100 % at a concentration of 500 mg/L. Furthermore, the study's results also confirmed that nano ZnO/OC-I₂ had greater antibacterial activity than nano ZnO/OC. Therefore, the nano ZnO/OC-I₂ complex had a great potential to use as an effective agent for jackfruit bronzing disease control.

Keywords: *Pantoea stewartii*, nano ZnO/OC, nano ZnO/OC-I₂, jackfruit.

Classification numbers: 1.1.3, 2.4.4.

1. INTRODUCTION

Nano ZnO has been studied for applications in solar cells [1, 2], sensors [3] and photodetectors [4, 5]. Nano ZnO also has antimicrobial and fungicidal activities [6,7], anti-inflammatory activity [8, 9], and wound healing acceleration [10], among others.

The use of of nanomaterials to efficiently manage harmful plant pathogens is currently receiving significant attention and development [11]. Nano ZnO is synthesized from low-cost raw materials through rational methods and processes, creating products that can be mass-produced [11]. Nano ZnO is biologically safer than Ag and CuO nanoparticles since it has low

toxicity to humans and the environment [12]. Recently, there have been some studies on the ability of nano ZnO to control of citrus canker on grapefruit trees [13] and eggplant bacterial wilt [14]. Furthermore, the use of ZnO nanoparticles in plants also improves the creation of antioxidants and defense enzymes while also promoting plant growth [15].

The antibacterial properties of nano ZnO are affected by particle morphology, size, surface defects, concentration and light exposure time [16]. Nano ZnO will have different morphologies depending on the synthesis method and the crystallization temperature, including flowerlike [17], flower-shaped, prism, rod-shaped, spherical-shaped, nanowires, nanoplates, and nanorods [16]. Many authors hypothesized the following mechanisms for ZnO nanoparticles antimicrobial resistance: disruption of the cell membrane [16,18], binding to proteins and DNA, generation of reactive oxygen species (ROS) [19], and disturbance of the processes of bacterial DNA amplification [20]. ZnO nanoparticles have also been shown to be capable of killing both gram-negative and gram-positive bacteria [21]. ZnO nanoparticles can be synthesized from zinc salts using the physicochemical sol-gel method [22,23], the sol-chemical method [24] or the mechanical method [25].

Chitosan is a β -1,4 linked polymer of glucosamine and lesser amounts of *N*-acetylglucosamine [26]. Chitosan has biological properties such as antibacterial, antifungal, anticancer, biodegradation, biocompatibility, stimulating plant disease resistance and wound healing [27]. Modification of the Mw of chitosan to prepare water-soluble OC using chemical, biological, or ionizing radiation methods has broadened its applicability. OC with low Mw, and water solubility has high antioxidant capacity, and can induce defensive responses in plant tissues to resist pathogens [28 - 30]. Because it is soluble in both acidic and alkaline media, OC is a potential biopolymer for stabilizing the nanosize of metals and metal oxides. Furthermore, because the synthesis reaction of ZnO nanoparticles by Zn^{2+} precipitation method is completed at alkaline pH, using chitosan with high Mw as stabilizer was inconvenient, as chitosan was precipitated when pH is adjusted above pKa \sim 6.5 [31, 32]. Therefore, some previous studies prepared nano ZnO/chitosan by mixing nano ZnO with chitosan solution, rather than using the sol-gel method [33, 34].

The antimicrobial activity of chitosan or OC can be increased by forming complexes with metal ions such as Cu^{2+} , Zn^{2+} , Fe^{2+} ... [35,36] or iodine ($KI + I_2$) [37], where the chitosan-iodine complex is a safe chemical that can be used as an antiseptic hydrogels and wound healing promoters, as well as an edible film for preserving food and fruits [38, 39]. Thus, a nano ZnO surface modified with OC- I_2 has the potential to be used as a microbial control agent and for post-harvest preservation of agricultural products. In this study, we use OC with low Mw and OC- I_2 complex as stabilizers for nano ZnO synthesis because they do not precipitate at alkaline pH.

Currently, the jackfruit bronzing diseases caused by gram-negative bacteria *Pantoea stewartii* is a serious disease wreaking havoc on super early jackfruit in Viet Nam. In Viet Nam, the jackfruit growing area, mainly Thai jackfruit was about 50,000 ha [40]. Over the years, super early Thai jackfruit has been infected by bronzing disease, which thrives during the rainy season. The initial survey results in Hau Giang province showed that 98.7 % of jackfruit plantations were infected, with disease incidence exceeding 10 % in 50.9 % of areas [41]. The bronzing disease causes the phenomenon of black rags on jackfruit [42].

Pantoea stewartii can host many plants, such as corn, rice, wheat, oats, and jackfruit [43]. It is gram-negative, facultative anaerobes, rod-shaped, non-flagellum, 1 - 2 μ m long, catalase-positive, whose colonies are yellow, slightly convex, and round with a size of 1 - 4 mm. The disease manifests as pulp and rags turning from yellow-orange to red, with rust spots, while the

external appearance of the fruit is unaffected [42, 44]. To minimize the damage of this disease, integrated control measures such as field sanitation, proper fertilization, disease-resistant varieties, rain cover for fruit to prevent rainwater from carrying bacteria into jackfruit, and pesticides use have been applied. However, the above measures have proven ineffective in controlling this disease.

In this report, we studied the preparation of nano ZnO/OC and nano ZnO/OC-I₂ and tested their *in vitro* the inhibitory effect against *P. stewartii* causing the jackfruit bronzing disease with the goal of using them as a disease-control agent in plants, particularly during the rainy season.

2. MATERIALS AND METHODS

2.1. Materials

Zinc oxide (99 %), and NaOH (96 %) were purchased from Xilong Scientific Co., Ltd. (Guangdong, China). KI, Luria Bertani Broth (LB), and lactic acid were purchased from Merck (Germany). Iodine was purchased from Himedia (India). OC with Mw ~3,300 g/mol, and degree of deacetylation (DD) of 91.36% was obtained from the Institute of Applied Materials Science (Viet Nam). *P. stewartii* bacteria was supplied by the Institute of Agriculture Science for Southern Viet Nam. All of the chemicals used in the study were analytical grade.

2.2. Preparation of OC-I₂ solution

Firstly, 12 g OC was dissolved in 150 mL distilled water in a 250 mL beaker to obtain OC solution. The KI³⁻ solution was prepared by dissolving 3.175 g I₂ and 4.15 g KI in 40 mL distilled water in a beaker. Then, the KI³⁻ solution was mixed into the OC solution and distilled water was added to prepare 200 mL of the OC-I₂ complex solution with total ingredient concentration of 96,625 mg/L including 60,000 mg/L OC, 15,875 mg/L I₂, and 20,750 mg/L KI.

2.3. Preparation of nano ZnO/OC colloidal solution

Dissolve 1.3 g ZnO and 3.6 g lactic acid in 50 mL distilled water to obtain a zinc lactate solution. The zinc lactate solution was mixed into 100 mL OC solution (120 g/L OC) solution. 9.5 g NaOH was dissolved in 30 mL distilled water and added dropwise into the Zn²⁺/OC solution that was placed on a magnetic stirrer, stirring constantly until the NaOH solution was completely added, then distilled water was added to make 200 mL. After the reaction was complete, an opalescent solution of Zn(OH)₂/OC was formed at pH 9. This solution was treated in an ultrasonic bath for 5 min at a frequency of 14 kHz and a power of 500W to obtain nano ZnO/OC solution with a total ingredient concentration of 66,500 mg/L containing 6,500 mg/L ZnO, and 60,000 mg/L OC.

2.4. Preparation of nano ZnO/OC-I₂ colloidal solution

1.3 g ZnO was put into a 250 mL beaker, followed by 20 mL water and 3.6 g lactic acid to obtain a zinc lactate solution. The zinc lactate solution was mixed into 100 mL the OC-I₂ solution (120 g/L OC, 31.75 g/L I₂, and 41.5 g/L KI) together with water to make 170 mL. 9.5 g NaOH was dissolved in 30 mL water and added dropwise to the Zn²⁺/OC-I₂ mixture, stirring constantly until the NaOH solution was completely added. After the reaction was completely, an opalescent solution of Zn(OH)₂/OC-I₂ was formed at pH 9. The beaker containing this solution

was placed for 5 min in an ultrasonic bath with a frequency of 14 kHz and a power of 500W to create ZnO/OC-I₂ nanoparticles with total ingredient concentration of 103,125 mg/L containing 6,500 mg/L ZnO, 60,000 mg/L OC, 15,875 mg/L I₂, and 20,750 mg/L KI.

2.5. Characterization of materials

The powders of OC, OC-I₂, nano ZnO/OC, and nano ZnO/OC-I₂ for characterization were prepared by vacuum drying at 60°C.

The Mw of OC was determined by GPC LC-20AD of Shimadzu - Japan, using a mixture of CH₃COOH 0.25 mol + CH₃COONa 0.25 mol as eluent. This device uses the RID 20A detector, shodex SB803 column HQ, using pullulan standard with Mw ranging from 780 to 10⁵ g/mol [45]. The ¹H-NMR spectrum of OC was carried out on a 500 Mhz Advance II HD nuclear magnetic resonance spectrometer of Bruker Biospin - Switzerland. The solvent was D₂O + CD₃COOD. DD of OC was calculated from the ¹H-NMR spectrum using formula (1) [46]:

$$DD (\%) = \left(1 - \frac{\frac{1}{3} \times H_{Ac}}{\frac{1}{6} \times H_{2-6}}\right) \times 100 \quad (1)$$

where H_{Ac} is the sum of the signal integral of the acetyl group's protons, H₂₋₆ is the integration of the proton signal from peak H₂ to H₆.

Transmission electron microscopy (TEM) images were captured using on a TEM S4800-NIHE - Japan. The X-ray diffraction (XRD) patterns were made using on an XRD D8 Advance-Bruker - Germany. The machine used Cu Kα (λ = 15,405 Å) radiation with a constant voltage of 30 mA, and 2θ diffraction angle from 5° to 80° [47].

2.6. In vitro assay of antibacterial activity

The antibacterial activity of the nano ZnO/OC and nano ZnO/OC-I₂ against *P. stewartii* was investigated using the agar diffusion method as proposed by to El-Masry et al. [48] and Wiegand et al. [49] with a slight modification. Sterile filter papers with a diameter of 6 mm were impregnated with 20 μL of tested substances at concentrations of 425, 450, 475 and 500 mg/L. Distilled water was used at control sample. Both test and control sterile filter papers were placed in petri dishes (diameter 90 mm) containing LB agar. Petri dishes were incubated at 37°C for 24 hours. The diameter of the inhibition zone was measured on the Interscience Scan 500 - France.

Besides, test tubes containing *P. stewartii* in LB medium (10⁸ cfu/mL) with test samples of studied materials at concentrations of 425, 450, 475 and 500 mg/L, while control sample without added material. All tubes were incubated at 37 °C for 24 hrs. The density of bacterial cells was determined by the colony counting method. Colonies were counted automatically on Interscience Scan 300, France. Finally, the inhibitory effect was calculated using formula (2):

$$\text{Inhibitory effect (\%)} = (N_0 - N) \times 100/N_0 \quad (2)$$

where N₀, and N (cfu/mL) are the number of survival bacteria in the control and the test samples, respectively [50].

All data were presented as mean ± standard deviation (SD). Oneway ANOVA was performed for each treatment with five replicates. The means were compared using the least significant difference (LSD) at 0.05 probability level (P ≤ 0.05).

3. RESULTS AND DISCUSSION

3.1. Characterization of ZnO/OC and ZnO/OC-I₂ nanomaterials

The Mw of OC was ~ 3,300 g/mol as determined by GPC based on retention time (Figure 1a). The DD was 91.36 % calculated from the ¹H-NMR spectrum (Figure 1b) according to formula (1), where H_{Ac} was 0.38 and H₂₋₆ was 8.8. In addition, the ¹H-NMR spectrum in Figure 1b showed that OC has typical resonance peaks for functional groups of chitosan [46].

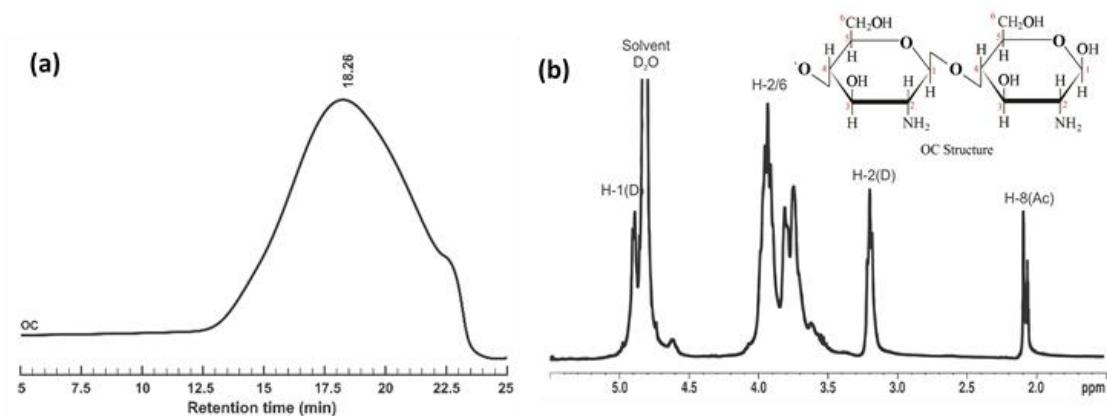


Figure 1. GPC chromatogram (a) and ¹H-NMR spectrum (b) of OC.

The average size of nano ZnO determined by TEM images (Figure 2) showed that the size of nano ZnO stabilized in OC-I₂ (~ 12.3 nm) was smaller than those stabilized in OC (~ 15.0 nm).

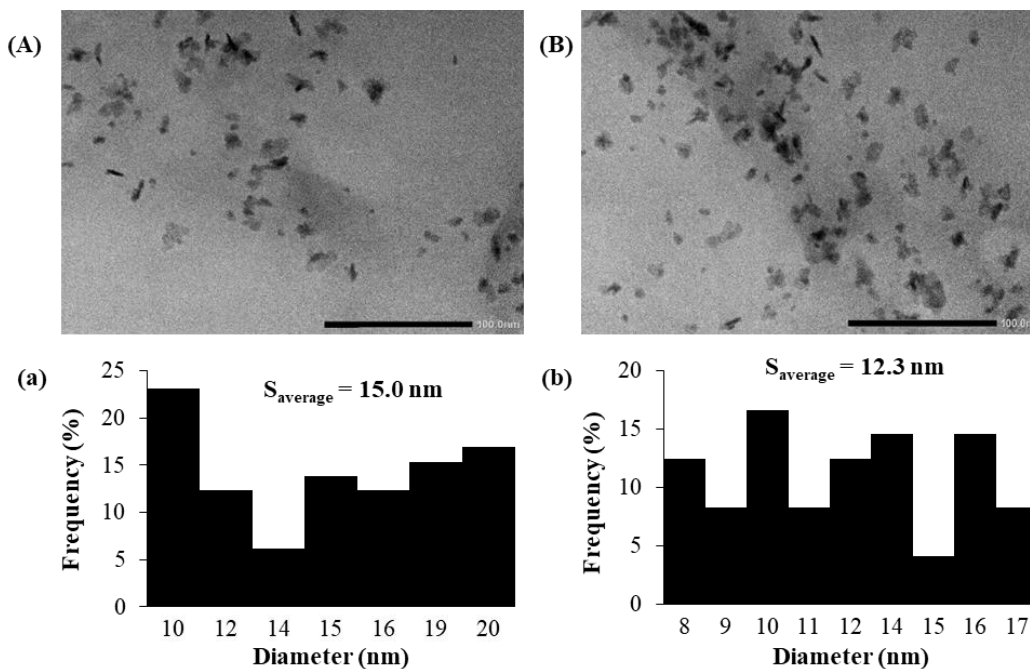


Figure 2. TEM images and particle size distributions of nano ZnO/OC (A, a) and nano ZnO/OC-I₂ complex (B, b)

The XRD pattern in Figure 3a showed that there was only a diffraction peak at $2\theta \sim 19^\circ$, while according to Podgorbunskikh et al. [51], chitosan with high Mw had two diffraction peaks at $2\theta \sim 10^\circ$ and 20° . The reason for this phenomenon is that when chitosan reduces Mw, the Intramolecular hydrogen bonds decrease, reducing the crystalline properties of chitosan. The XRD pattern in Figure 3b showed that OC-I₂ was almost amorphous, the complex between OC and iodide had lost the crystalline properties of OC, which was consistent with Shigeno et al. [52]. Figures 3c and 3d showed that zinc exists as ZnO with a wurtzite crystal structure with characteristic diffraction peaks at $2\theta \sim 31.8^\circ$, 34.5° , 36.3° , 47.6° , 56.7° , 63.1° , and 68.1° corresponding to reflection planes (100), (002), (101), (102), (110), (103) and (112), respectively [53].

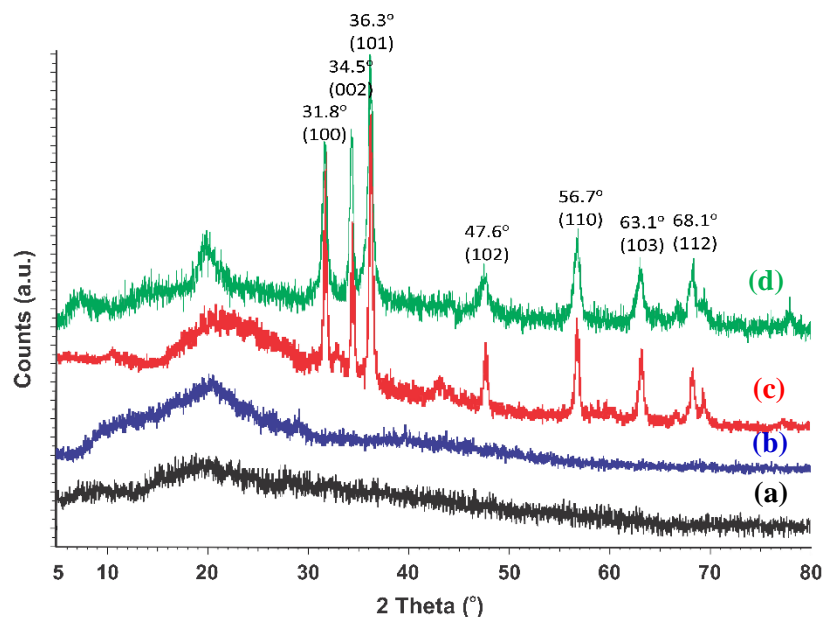


Figure 3. XRD patterns of OC (a), OC-I₂ (b), nano ZnO/OC (c) and nano ZnO/OC-I₂ (d).

3.2. *In vitro* assay of antibacterial activity

The diameters of the inhibition zone against *P. stewartii* of the studied samples are presented in Table 1. Figure 4 and Table 1 showed that OC with Mw of $\sim 3,300$ g/mol exhibited no inhibition zone against *P. stewartii* at all experimental concentrations. It suggested that OC with low Mw had a weak ability to kill bacteria through a direct mechanism, as observed in studies conducted by some previous studies [26, 30]. However, OC with low Mw had high antioxidant properties and the ability to induce defense reactions in plant tissues, including the synthesis of phytoalexin, accumulating of phenolic compounds, increasing tyrosine ammonia lyase, phenylalanine ammonia-lyase, polyphenol oxidase, peroxidase and chitinase activities [28].

Table 1. The diameter of the inhibition zone against *P. stewartii* of OC, OC-I₂, nano ZnO/OC, and nano ZnO/OC-I₂ after 24 hours.

Materials	Conc. (mg/L)	Diameter of the inhibition zone (mm)	Materials	Conc. (mg/L)	Diameter of the inhibition zone (mm)
OC	425	0	Nano ZnO/OC	425	10.2 ± 0.7 ^a
	450	0		450	16.7 ± 1.2 ^b
	475	0		475	17.9 ± 0.7 ^{bc}
	500	0		500	18.9 ± 1.0 ^c
LSD _{0.05}		-			1.3
OC-I ₂	425	5.3 ± 0.6 ^a	Nano ZnO/OC-I ₂	425	16.1 ± 0.9 ^a
	450	10.2 ± 1.1 ^b		450	19.5 ± 1.0 ^b
	475	10.5 ± 0.9 ^b		475	20.7 ± 1.3 ^b
	500	13.3 ± 1.2 ^c		500	29.1 ± 1.2 ^c
LSD _{0.05}		1.4			1.5

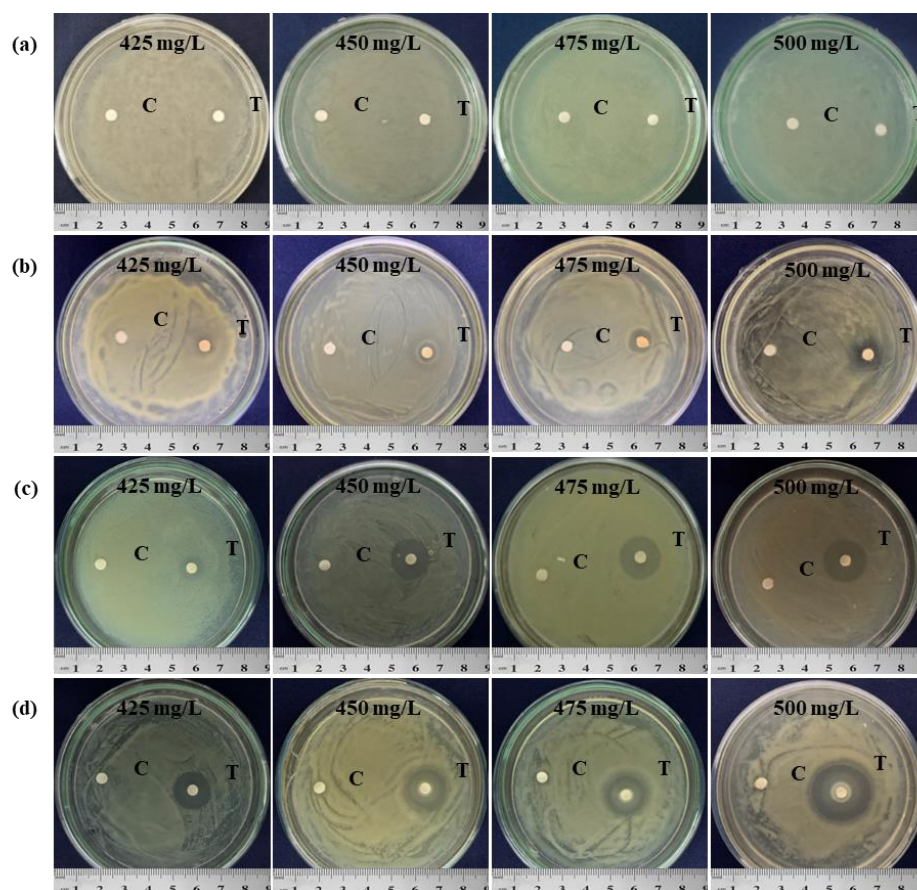


Figure 4. The diameter of the inhibition zone against *P. stewartii* of OC (a), OC-I₂ (b), nano ZnO/OC (c), and nano ZnO/OC-I₂ (d) after 24 hours. (Note: C is control and T is treatment).

For the OC-I₂, an inhibition zone against *P. stewartii* did appear, with inhibition zone diameters ranging from 5.3 to 13.3 mm after 24 hours. Therefore, the interaction of I₃⁻ and OC showed antibacterial effects. The inhibition zone of OC-I₂ was, however, smaller than that of nano ZnO/OC and nano ZnO/OC-I₂. At concentrations of 425, 450, 475 and 500 mg/L, the diameter of the inhibition zone for *P. stewartii* of nano ZnO/OC was 10.2, 16.7, 17.9 and 18.9 mm, respectively, and for nano ZnO/OC-I₂ was 16.1, 19.5, 20.7 and 29.1 mm, respectively. These results demonstrated that nano ZnO at low concentration of 31 mg/L (equiv. 500 mg/L nano ZnO/OC-I₂) when stabilized in OC-I₂ had higher antibacterial activity than nano ZnO at a concentration of 49 mg/L (equiv. 500 mg/L nano ZnO/OC) stabilized in OC. This finding was also consistent with Gudkov et al. [54], who reported that ZnO nanoparticles had antibacterial properties at low concentrations ranging from 0.16 to 5.0 mM (equiv. 12,96 - 405 mg/L).

Based on the results of antibacterial activity through the diameter of the inhibition zone, we further conducted the experiment to determine the inhibitory effect of nano ZnO/OC and nano ZnO/OC-I₂ for *P. stewartii*. The results are presented in Table 2.

Table 2. The inhibitory effect of nano ZnO/OC, and nano ZnO/OC-I₂ against *P. stewartii* after 24 hours.

Active ingredient concentrations	Nano ZnO/OC		Nano ZnO/OC-I ₂	
	Density (10 ⁸ cfu/mL)	Inhibitory effect (%)	Density (10 ⁸ cfu/mL)	Inhibitory effect (%)
Control	4.24 ± 0.51 ^a	-	4.24 ± 0.51 ^a	-
425 mg/L	2.18 ± 0.43 ^b	48.11	1.40 ± 0.11 ^b	66.98
450 mg/L	1.98 ± 0.30 ^b	57.08	0.82 ± 0.07 ^c	80.66
475 mg/L	1.73 ± 0.28 ^b	63.92	0.51 ± 0.15 ^c	87.97
500 mg/L	0.64 ± 0.24 ^c	84.91	0 ^d	100
LSD _{0.05}	0.51	-	0.34	-

The mean values in a column with the same letter are not significant difference at $P \leq 0.05$

Table 2 showed that the inhibitory effect of nano ZnO/OC against *P. stewartii* at a concentration of 500 mg/L after 24 hours was 84.91 %, which was statistically significantly higher than the other treatments. Meanwhile, the inhibitory effect of nano ZnO/OC at concentrations ranging from 425 to 475 mg/L showed no significant difference. For nano ZnO/OC-I₂, at a concentration of 500 mg/L, *P. stewartii* was completely inhibited. The inhibitory effect of nano ZnO/OC-I₂ was higher than that of nano ZnO/OC when used at the same concentration of 500 mg/L. This phenomenon could be explained by the synergistic effect of the complex's individual substances.

Recently, studies on ZnO nanoparticles's antibacterials activity in plants were also published. For example, Nandhini et al. [55] discovered that ZnO nanoparticles at a concentration of 500 ppm were effective against *Sclerospora graminicola*, which causes downy mildew disease on pearl millet. Vera-Reyes et al. [56] reported that ZnO nanoparticles at a concentration of 700 mg/L inhibited 90 % of *Clavibacter michiganensis*, and at a concentration of 1000 mg/L inhibited 67 % of *Pseudomonas syringae* in *in vitro* tests. As far as we know, no previous research on the use of nano ZnO to inhibit *P. stewartii* has been published.

4. CONCLUSION

In this work, the nano ZnO/OC and nano ZnO/OC-I₂ were successfully prepared using the sol-gel method. The *in vitro* antibacterial activity of these nanomaterials against *P. stewartii* showed that nano ZnO/OC-I₂ had a greater antibacterial effect than nano ZnO/OC. The results also proved that the combination of nano ZnO, OC, and iodine produced a nano complex with enhanced antibacterial properties. Therefore, these synthesized nano ZnO/OC and nano ZnO/OC-I₂ have the potential to be used as an effective plant disease control agent, particularly for the jackfruit bronzing disease in Viet Nam.

Acknowledgements. This research was funded by the priority scientific directions of the Vietnam Academy of Science and Technology (grant No: VAST03.05/22-23).

CRedit authorship contribution statement. Phong N. T. H., Du B. D.: Designing the simulations and experiments; Phong N. T. H., Tho T. P.: Performing the experiments; Tuan L. N. A.: Analyzing data; Du B. D., Hien N. Q.: Writing manuscript; Hien N. Q.: Editing the manuscript. We confirm that the manuscript has been read and approved by all named authors.

Declaration of competing interest. The authors declare that they have no known competing financial interests or personal relationships that could have appeared to influence the work reported in this paper.

REFERENCES

1. Beek W. J., Wienk M. M., and Janssen R. A. - Efficient hybrid solar cells from zinc oxide nanoparticles and a conjugated polymer. *Adv. Mater.*, **16** (12) (2004) 1009-1013. doi.org/10.1002/adma.200306659.
2. Suliman A. E., Tang Y., and Xu L. - Preparation of ZnO nanoparticles and nanosheets and their application to dye-sensitized solar cells. *Sol. Energy Mater. Sol. Cells*, **91** (18) (2007) 1658-1662. doi.org/10.1016/j.solmat.2007.05.014.
3. Baruwati B., Kumar D. K., and Manorama S. V. - Hydrothermal synthesis of highly crystalline ZnO nanoparticles: A competitive sensor for LPG and EtOH. *Sens. Actuators B: Chem.*, **119** (2) (2006) 676-682. doi.org/10.1016/j.snb.2006.01.028.
4. Vaseem M., Umar A., and Hahn Y. B. - ZnO nanoparticles: Growth, properties, and applications. In: Umar A., and Hahn Y. B. - *Metal oxide nanostructures and their applications*, American Scientific Publishers, American, (2010) pp. 1-36.
5. Chang S. P., and Chen K. J. - Zinc oxide nanoparticle photodetector. *J. Nanomater.*, **2012** (2012) 602398. doi.org/10.1155/2012/602398.
6. Houšková V., Štengl V., Bakardjieva S., Murafa N., Kalendova A., and Opluštil F. - Zinc oxide prepared by homogeneous hydrolysis with thioacetamide, its destruction of warfare agents, and photocatalytic activity. *J. Phys. Chem. A*, **111** (20) (2007) 4215-4221. doi.org/10.1021/jp070878d.
7. Dadi R., Azouani R., Traore M., Mielcarek C., and Kanaev A. - Antibacterial activity of ZnO and CuO nanoparticles against gram positive and gram negative strains, *Mater. Sci. Eng.: C*, **104** (2019) 109968. doi.org/10.1016/j.msec.2019.109968.
8. Nagajyothi P. C., Cha S. J., Yang I. J., Sreekanth T. V. M., Kim K. J., and Shin H. M. - Antioxidant and anti-inflammatory activities of zinc oxide nanoparticles synthesized using *Polygala tenuifolia* root extract. *J. Photochem. Photobiol. B: Biol.*, **146** (2015) 10-17. doi.org/10.1016/j.jphotobiol.2015.02.008.

9. Agarwal H., and Shanmugam V. - A review on anti-inflammatory activity of green synthesized zinc oxide nanoparticle: Mechanism-based approach. *Bioorg. Chem.*, **94** (2020) 103423 doi.org/10.1016/j.bioorg.2019.103423.
10. Mishra P. K., Mishra H., Ekielski A., Talegaonkar S., and Vaidya B. - Zinc oxide nanoparticles: A promising nanomaterial for biomedical applications. *Drug Discov. Today*, **22** (12) (2017) 1825-1834. doi.org/10.
11. Kalia A., Abd-Elsalam K. A., and Kuca K. - Zinc-based nanomaterials for diagnosis and management of plant diseases: Ecological safety and future prospects. *J. Fungi*, **6** (4) (2020) 222. doi.org/10.3390/jof6040222.
12. Zhang W., Liu X., Bao S., Xiao B., and Fang T. - Evaluation of nano-specific toxicity of zinc oxide, copper oxide, and silver nanoparticles through toxic ratio. *J. Nanopart. Res.*, **18** (2016) 1-13. doi.org/10.1007/s11051-016-3689-2.
13. Graham J. H., Johnson E. G., Myers M. E., Young M., Rajasekaran P., Das S., and Santra S. - Potential of nano-formulated zinc oxide for control of citrus canker on grapefruit trees. *Plant Dis.*, **100** (12) (2016) 2442-2447. doi.org/10.1094/pdis-05-16-0598-re.
14. Khan M., and Siddiqui Z. A. - Zinc oxide nanoparticles for the management of *Ralstonia solanacearum*, *Phomopsis vexans* and *Meloidogyne incognita* incited disease complex of eggplant. *Indian Phytopathol.*, **71** (3) (2018) 355-364. doi.org/10.1007/s42360-018-0064-5.
15. Elsharkawy M., Derbalah A., Hamza A., and El-Shaer A. - Zinc oxide nanostructures as a control strategy of bacterial speck of tomato caused by *Pseudomonas syringae* in Egypt. *Environ. Sci. Pollut. Res.*, **27** (16) (2020) 19049-19057. doi.org/10.1007/s11356-018-3806-0.
16. Sirelkhatim A., Mahmud S., Seeni A., Kaus N. H. M., Ann L. C., Bakhori S. K. M., Hasan H., and Mohamad D. - Review on zinc oxide nanoparticles: Antibacterial activity and toxicity mechanism. *Nano Micro Lett.*, **7** (3) (2015) 219-242. doi.org/10.1007/s40820-015-0040-x.
17. Zhang J., Sun Yin Su H., and Liao Yan C. - Control of ZnO morphology via a simple solution route, *Chem. Mater.*, **14** (10) (2002) 4172-4177. doi.org/10.1021/cm020077h.
18. Liu Y. J., He L. L., Mustapha A., Li H., Hu Z. Q., and Lin M. S. - Antibacterial activities of zinc oxide nanoparticles against *Escherichia coli* O157:H7. *J. Appl. Microbiol.*, **107** (4) (2009) 1193-1201. doi.org/10.1111/j.1365-2672.2009.04303.x.
19. Gold K., Slay B., Knackstedt M., and Gaharwar A. K. - Antimicrobial activity of metal and metal-oxide based nanoparticles. *Adv. Ther.*, **1** (3) (2018) 1700033. doi.org/10.1002/adtp.201700033.
20. Xie Y., He Y., Irwin P. L., Jin T., and Shi X. - Antibacterial activity and mechanism of action of zinc oxide nanoparticles against *Campylobacter jejuni*. *Appl. Environ. Microbiol.*, **77** (7) (2011) 2325-2331. doi.org/10.1128/AEM.02149-10.
21. Yusof N. A. A., Zain N. M., and Pauzi N. - Synthesis of ZnO nanoparticles with chitosan as stabilizing agent and their antibacterial properties against gram-positive and gram-negative bacteria. *Int. J. Biol. Macromol.*, **124** (2019) 1132-1136. doi.org/10.1016/j.ijbiomac.2018.11.228.

22. Azam A., Ahmed A. S., Oves M., Khan M. S., Habib S. S., and Memic A. - Antimicrobial activity of metal oxide nanoparticles against gram-positive and gram-negative bacteria: A comparative study. *Int. J. Nanomed.*, **7** (2012) 6003-6009. doi.org/10.2147/IJN.S35347.
23. Alias S. S., and Mohamad A. A. - ZnO Nanocrystalline Metal Oxide semiconductor via sol gel method, in: Alias S. S., and Mohamad A. A. (Eds.), *Synthesis of zinc oxide by sol-gel method for photoelectrochemical cells*, Springer, Singapore, 2014, pp.1-7. doi.org/10.1007/978-981-4560-77-1.
24. Souza R. C. D., Haberbeck L. U., Riella H. G., Ribeiro D. H., and Carciofi B. A. - Antibacterial activity of zinc oxide nanoparticles synthesized by solochemical process. *Braz. J. Chem. Eng.*, **36** (2019) 885-893. doi.org/10.1590/0104-6632.20190362s20180027.
25. Tran N., Mir A., Mallik D., Sinha A., Nayar S., and Webster T. J. - Bactericidal effect of iron oxide nanoparticles on *Staphylococcus aureus*. *Int. J. Nanomed.*, **5** (2010) 277-283. doi.org/10.2147/IJN.S9220.
26. Du D. X., and Vuong B. X. - Study on preparation of water-soluble chitosan with varying molecular weights and its antioxidant activity. *Adv. Mater. Sci. Eng.*, **2019** (2019) 8781013. doi.org/10.1155/2019/8781013.
27. Dai T., Tanaka M., Huang Y. Y., and Hamblin M. R. - Chitosan preparations for wounds and burns: Antimicrobial and wound-healing effects. *Expert Rev. Anti-Infect. Ther.*, **9** (7) (2011) 857-879. doi.org/10.1586/eri.11.59.
28. Li P., Cao Z., Wu Z., Wang X., and Li X. - The effect and action mechanisms of oligochitosan on control of stem dry rot of *Zanthoxylum bungeanum*. *Int. J. Mol. Sci.*, **17** (7) (2016) 1044. doi.org/10.3390/ijms17071044.
29. Thuy N. N., Quy H. D., Duy N. N., Hien N. Q., and Hai N. D. - Preparation, characterization, and antioxidant activity of water-soluble oligochitosan. *Green Process. Synth.*, **6** (5) (2017) 461-468. doi.org/10.1515/gps-2016-0126.
30. Qian J., Wang Q., Chen Y., Mo C., Liang C., and Guo H. - The correlation of molecule weight of chitosan oligomers with the corresponding viscosity and antibacterial activity. *Carbohydr. Res.*, **530** (2023) 108860. doi.org/10.1016/j.carres.2023.108860.
31. Wang Q. Z., Chen X. G., Liu N., Wang S. X., Liu C. S., Meng X. H., and Liu C. G. - Protonation constants of chitosan with different molecular weight and degree of deacetylation. *Carbohydr. Polym.*, **65** (2) (2006) 194-201. doi.org/10.1016/j.carbpol.2006.01.001.
32. Mohammed M. A., Syeda J. T. M., Wasan K. M., and Wasan E. K. - An overview of chitosan nanoparticles and its application in non-parenteral drug delivery. *Pharm.* **9** (4) (2017) 53-78. doi.org/10.3390/pharmaceutics9040053.
33. Mustika R., and Wardana A. - Nanocomposite coating based on chitosan and ZnO nanoparticles to maintain the storage quality of meatball. *Food Res.* **4** (2020) 1867-1870. doi.org/10.26656/fr.2017.4(6).169.
34. Zhang X., Zhang Z., Wu W., Yang J., and Yang Q. - Preparation and characterization of chitosan/nano-ZnO composite film with antimicrobial activity. *Bioprocess Biosyst. Eng.* **44** (6) (2021) 1193-1199. doi.org/10.1007/s00449-021-02521-x.

35. Pillai C. K., Paul W., and Sharma C. P. - Chitin and chitosan polymers: Chemistry, solubility and fiber formation. *Prog. Polym. Sci.*, **34** (7) (2009) 641-678. doi.org/10.1016/j.progpolymsci.2009.04.001.
36. Bondarenko O., Juganson K., Ivask A., Kasemets K., Mortimer M., and Kahru A. - Toxicity of Ag, CuO and ZnO nanoparticles to selected environmentally relevant test organisms and mammalian cells in vitro: A critical review. *Arch. Toxicol.*, **87** (7) (2013) 1181-1200. doi.org/10.1007/s00204-013-1079-4.
37. Mallick S., Sharma S., Banerjee M., Ghosh S. S., Chattopadhyay A., and Paul A. - Iodine-stabilized Cu nanoparticle chitosan composite for antibacterial applications. *ACS Appl. Mater. Interfaces*, **4** (3) (2012) 1313-1323. doi.org/10.1021/am201586w.
38. Hassan E. M. - Ionic chitosan-iodine complexes: Antiseptic hydrogels and wound healing promoters. U.S. Patent No. US6521243B2, Washington, DC: U.S. Patent and Trademark Office, 2003.
39. Limchoowong N., Sricharoen P., Techawongstien S., Chanthai S. - An iodine supplementation of tomato fruits coated with an edible film of the iodide-doped chitosan. *Food Chem.*, **200** (2016) 223-229. doi.org/10.1016/j.foodchem.2016.01.042.
40. Tri M. V., Hoa N. V., Chau N. M., Pane A., Faedda R., De Patrizio A., Schena L., Olsson C. H. B., Wright S. A. I, Ramstedt M., et al. - Decline of jackfruit (*Artocarpus heterophyllus*) incited by *Phytophthora palmivora* in Viet Nam. *Phytopathol. Mediterr.*, **54** (2) (2015) 275-280. doi.org/10.14601/Phytopathol_Mediterr-15008.
41. Chung M. D., Duc T. H., Kieu N. T., Phuong N. D., Ha N. T., Canh N. X., Giang N. V., Hien P. H., Yen N. H., and Duc N. T. - Pests and diseases survey on jackfruit trees in Hau Giang province. *Mon. J.*, **6** (139) (2022) 79-86. doi.org/10.32945/atr3612.2014.
42. Gapasin R. M., Garcia R. P., Advincula C. T., De la Cruz C. S., and Borines L. M. - Fruit bronzing: a new disease affecting jackfruit caused by (smith) mergaert *Pantoea stewartii* et al. *Ann. Trop. Res.*, **36** (1) (2014) 17-31.
43. Jeger M., Bragard C., Candresse T., and Chatzivassiliou E., Dehnen-Schmutz K., Gilioli G., Caffier D. - Pest categorisation of *Pantoea stewartii* subsp. *stewartii*. *EFSA J.*, **16** (7) (2018) e05356. doi.org/10.2903/j.efsa.2018.5356.
44. Ibrahim R., Ismail S. I., Ina-Salwany M. Y., and Zulperi D. - Biology, diagnostics, pathogenomics and mitigation strategies of jackfruit-bronzing bacterium *Pantoea stewartii* subspecies *stewartii*: What do we know so far about this culprit?. *Hortic.*, **8** (8) (2022) 702. doi.org/10.3390/horticulturae8080702.
45. Duy N. N., Phu D. V., Anh N. T., and Hien N. Q. - Synergistic degradation to prepare oligochitosan by γ -irradiation of chitosan solution in the presence of hydrogen peroxide. *Radiat. Phys. Chem.*, **80** (7) (2011) 848-853. doi.org/10.1016/j.radphyschem.2011.03.012.
46. Lavertu M., Xia Z., Serreqi A. N., Berrada M., Rodrigues A., Wang D., Buschmann M. D., and Gupta A. - A validated $^1\text{H-NMR}$ method for the determination of the degree of deacetylation of chitosan. *J. Pharm. Biomed. Anal.*, **32** (6) (2003) 1149-1158. doi.org/10.1016/S0731-7085(03)00155-9.
47. Dey S. C., Al-Amin M., Rashid T. U., Sultan M. Z., Ashaduzzaman M., Sarker M., and Shamsuddin S. M. - Preparation, characterization and performance evaluation of chitosan as an adsorbent for remazol red. *Int. J. Latest Res. Eng. Technol.*, **2** (2) (2016) 52-62.

48. El-Masry R. M., Talat D., Hassoubah S. A., Zabermaawi N. M., Eleiwa N. Z., Sherif R. M., Abourehab M. A. S., Abdel-Sattar R. M., Gamal M., Ibrahim M. S., et al. - Evaluation of the antimicrobial activity of ZnO nanoparticles against enterotoxigenic *Staphylococcus aureus*. *Life*, **12** (10) (2022) 1662. doi.org/10.3390/life12101662.
49. Wiegand I., Hilpert K., and Hancock R. E. - Agar and broth dilution methods to determine the minimal inhibitory concentration (MIC) of antimicrobial substances. *Nat. Protoc.*, **3** (2) (2008) 163-175. doi.org/10.1038/nprot.2007.521.
50. Du B. D., Phu D. V., Quoc L. A., and Hien N. Q. - Synthesis and investigation of antimicrobial activity of Cu₂O nanoparticles/zeolite. *J. Nanopart.*, **2017** (2017) 7056864. doi.org/10.1155/2017/7056864.
51. Podgorbunskikh E., Kuskov T., Rychkov D., Lomovskii O., and Bychkov A. - Mechanical amorphization of chitosan with different molecular weights. *Polym.*, **14** (20) (2022) 4438. doi.org/10.3390/polym14204438.
52. Shigeno Y., Kondo K., and Takemoto K. - Functional monomers and polymers, 74. Physico-chemical study on the chitosan-iodine complexes. *Die Angew. Makromol. Chem.*, **91** (1) (1980) 55-67. doi.org/10.1002/apmc.1980.050910105.
53. Thanh N. N., Thinh N. N., anh Anh N. V. - In situ synthesis and characterization of ZnO/chitosan nanocomposite as an adsorbent for removal of congo red from aqueous solution. *Adv. Polym. Technol.*, **2020** (2020) 3892694. doi.org/10.1155/2020/3892694.
54. Gudkov S. V., Burmistrov D. E., Serov D. A., Rebezov M. B., and Semenova A. A., Lisitsyn A. B. - A mini review of antibacterial properties of ZnO nanoparticles. *Front. Phys.*, **9** (2021) 641481. doi.org/10.3389/fphy.2021.641481.
55. Nandhini M., Rajini S. B., Udayashankar A. C., Niranjana S. R., Lund O. S., Shetty H. S., and Prakash H. S. - Biofabricated zinc oxide nanoparticles as an eco-friendly alternative for growth promotion and management of downy mildew of pearl millet. *Crop Prot.*, **121** (2019) 103-112. doi.org/10.1016/j.cropro.2019.03.015.
56. Vera-Reyes I., Esparza-Arredondo I. J. E., Lira-Saldivar R. H., Granados-Echegoyen C. A., Alvarez-Roman R., Vásquez-López A., Santos-Villarreal G., and Díaz-Barriga Castro E. - *In vitro* antimicrobial effect of metallic nanoparticles on phytopathogenic strains of crop plants, *J. Phytopathol.*, **167** (2019) 461-469. doi.org/10.1111/jph.12818.

Graphic of TOC

